Low-frequency phonon dynamics of the $C_{60}(111)$ surface

A. Glebov, V. Senz, and J. P. Toennies
Max-Planck-Institut für Strömungsforschung, Bunsenstrasse 10, D-37073 Göttingen, Germany

Ph. Lambin, G. Gensterblum, P. Senet, and A. A. Lucas
Department of Physics, Facultés Universitaires Notre-Dame de la Paix, 61 Rue de Bruxelles, B-5000 Namur, Belgium

(Received 9 June 1997)

High-quality C_{60} films, with a thickness of about 100 Å, were epitaxially grown on *in vacuo* cleaved GeS(001) single crystal surfaces and characterized with helium atom diffraction. Phonon dispersion curves of the $C_{60}(111)$ surface were obtained from high-resolution inelastic helium atom time-of-flight (TOF) spectra. Pronounced inelastic peaks corresponding to the Rayleigh modes and to the frustrated rotations (librations) of the C_{60} molecules were observed along the $\langle 110\rangle$ and $\langle 112\rangle$ directions. The anharmonicity of the librations was found to be slightly larger than in the bulk C_{60}. The contribution of the C_{60} vibrations (without librons) to the inelastic TOF peak intensities was estimated from lattice dynamic calculations based on the intermolecular potential of Girifalco [J. Phys. Chem. **92**, 858 (1992)]. [S0163-1829(97)08939-X]

I. INTRODUCTION

The study of the dynamical properties of C_{60} fullerites is a subject of intense activity,[1] motivated by the further interest of explaining the superconductivity of alkali-doped fullerites. Whereas the phonon structure is well understood in the C_{60} *bulk* material,[2] much less is known about its *surface* dynamics. The present work aims at filling this gap by providing results on the low-frequency lattice modes corresponding to the vibrational degrees of freedom of the molecule as a whole (phonons) and the rotational degrees of freedom (librons).[3,4]

At room temperature, the crystal has a face-centered-cubic (fcc) structure, where the C_{60} molecules rotate freely. With decreasing temperature, the rotational degrees of freedom of the C_{60} molecules becomes more and more hindered and the solid undergoes an orientational ordering transition from the fcc phase to the simple cubic (sc) structure at 260 K in the bulk.[5] At the surface where the molecules have fewer neighbors to interact with, low-energy electron diffraction (LEED),[6] x-ray diffraction,[7] and helium atom scattering (HAS),[8] all reveal that the surface phase transition occurs at $T_c \approx 235$ K, which is about 25 K lower than in the bulk.

According to molecular-dynamics calculations, the bulk density of states of the C_{60} intermolecular modes extends up to an energy of 7.6 meV and has two peaks with strong libronic character at 2.3 and 3.7 meV.[9] By means of neutron scattering on polycrystaline C_{60}, Neumann *et al.*[10] detected a librational motion of the C_{60} molecules at an energy that shifted from 2.8 meV at 20 K down to 2.0 meV at 250 K, while getting broader as the temperature increased. Pintschovius *et al.*[11] also measured the C_{60} phonon dispersion curves with inelastic neutron scattering in polycrystaline samples and reported on slightly dispersive librational modes at around 2.4, 3.6, and 4.6 meV at $T_{\mathrm{surf}}=200$ K. In high-resolution Raman spectroscopy at 77 K, Horoyski, Thewalt, and Anthony[12] observed three sharp peaks at 2.2, 2.6, and 3.0 meV, as well as weaker and broader bands at 4.0, 5.1, and 6.1 meV. The four lower modes have been identified as the allowed Raman active modes (librons) of the sc phase.[13] The two latter modes (5.1 and 6.1 meV) were attributed to two of the four infrared-active phonons,[12] which were previously measured by infrared spectroscopy at 5.0 and 6.8 meV.[14,15] On the other hand, far-infrared transmission spectra of C_{60} have also revealed peaks at 1.0, 1.6, 2.2, and 2.7 meV.[16]

The effects of the missing C_{60}-C_{60} bonds at the surface and other possible surface effects on the phonon-libron spectrum of the fullerite are unknown. An initial attempt at measuring the low-energy phonon dispersion curves of the $C_{60}(111)$ surface with HAS was first reported by Schmicker *et al.*[17] The 1–2-ML-thick C_{60} films were grown on a mica substrate at room temperature. However, due to a rather poor quality of the films, the authors were only able to obtain weak indications of two modes at around 1.5 and 3 meV, with an energy accuracy of about 30% and no clear evidence for the Rayleigh mode was found. This surface acoustical wave has recently been detected by means of surface Brillouin scattering on a (111) film of C_{60} on Ni(110),[18] which revealed that the phase velocity of this mode (≈ 1460 m/s) was somewhat dependent on the azimuthal direction.

In this paper, high-resolution HAS measurements of the C_{60} surface phonon dispersion curves are presented. In addition to two librational modes of the $C_{60}(111)$ surface, the Rayleigh wave was also observed. From the measured temperature dependence of the libron frequencies the surface anharmonicity constants were determined. The phonons dispersion curves—including the Rayleigh wave—were computed for a slab using a 12-6 Lennard-Jones interatomic potential, for which there is no librational force constant, since the molecules are viewed as spherical.[19] However, as the libron modes are weakly dispersive in bulk C_{60}, they can be easily projected on these calculated surface phonon bands. This simplified description was adopted here since in addition to providing a rather good agreement with experimental data, it is much less time-expensive than a ''brute force'' surface dynamics calculation for a potential which accounts for atom-atom interaction and was proposed for bulk C_{60}.[3,4,9]

II. EXPERIMENTAL SETUP AND FILM GROWTH

The helium atom scattering apparatus, used in this work, is described in detail elsewhere[20,21] and, thus, is only briefly presented. A highly monoenergetic He beam (full width at half maximum $\Delta v/v \approx 1\%$, $\Delta E/E \approx 2\%$) is produced by a free jet expansion through a 10-μm aperture into vacuum. The beam is then chopped and after scattering from the crystal surface, the He atoms pass through three differentially pumped stages and are detected at a distance of about 140 cm from the target by a magnetic mass spectrometer operating in the ion-counting mode. The angle between incoming and outgoing beams Θ_{SD} is fixed at 90 ° so that the incident Θ_i and final Θ_f scattering angles, measured with respect to the surface normal, are given by $\Theta_{SD}=\Theta_i+\Theta_f=90°$. Different momentum transfers ΔK parallel to the surface were probed by polar rotation of the sample around an axis perpendicular to the sagittal plane and for elastic scattering are given by $\Delta K = k_i(\sin\Theta_f - \sin\Theta_i)$, where k_i is the incident wave vector. The inelastic scattering experiments reported here were carried out at an incident beam energy $E_i = 13.5$ meV, corresponding to an incident wave vector $k_i = 5.2$ Å^{-1}.

The GeS crystals, used as substrates for epitaxially grown C_{60} films, were attached on a metal plate that was mounted on the sample holder of the manipulator. The GeS(001) surface was cleaved *in situ* at pressures in the 10^{-6} mbar range by means of a piece of scotch tape connected by a wire to a rotary feed through. After the cleavage, the scotch tape was removed though a vacuum lock from the scattering chamber, which then was baked out for about 20 h at $T=200$ °C. During the measurements, the base pressure was in the middle 10^{-11} mbar range. The final annealing of the crystal to 550 K for about 2 h resulted in a significant improvement of the surface as indicated by an increase of the He specular peak intensity from 1×10^5 counts/s (cps) to 6×10^6 cps accompanied by a substantial reduction in the width of the diffraction peaks. The temperature of the crystal was regulated via cooling with the liquid-helium cold finger or heating with a resistively heated filament mounted immediately behind the sample holder. The crystal temperature was measured by two NiCr/Ni thermocouples pressed to the metal plate behind the sample. The temperature measurements are estimated to be accurate to within 1–2 °C.

The technique of C_{60} film growth on GeS(001) is surveyed in detail in Ref. 23. The chromatographically purified C_{60} powder [purity >99.9% (Ref. 22)] was loaded into a graphite crucible of a Knudsen cell (WA technology, UK), located about 15 cm from the sample, and carefully outgassed, first for 12 h at a temperature of 650 K, and then for 1 h at 690 K. C_{60} was evaporated at a source temperature $T_{cell}=700$ K on the GeS surface at $T_{surf}=470$ K. Since this substrate temperature is only 20 K lower than the desorption temperature of the film, $T_{des}=490$ K, there is sufficient mobility of the adsorbed C_{60} molecules to assure formation of well-ordered and nearly defect-free films, which were found to remain stable for several days at temperatures up to $T_{surf}=470$ K. By heating the sample for several hours at $T_{surf}=550$ K the C_{60} layer was completely desorbed and the original quality of the substrate was restored. An extended HAS investigation of the film growth mechanisms as well as the microscopic quality of the films has recently been reported[8] and indicate that the C_{60} films grow on the GeS(001) surface according to the ''step-flow'' growth mode. Furthermore, the results of the helium atom diffraction demonstrated that the long- and short-range order of the epitaxially grown C_{60} films was comparable with that of the cleaved *in situ* GeS substrate surface.

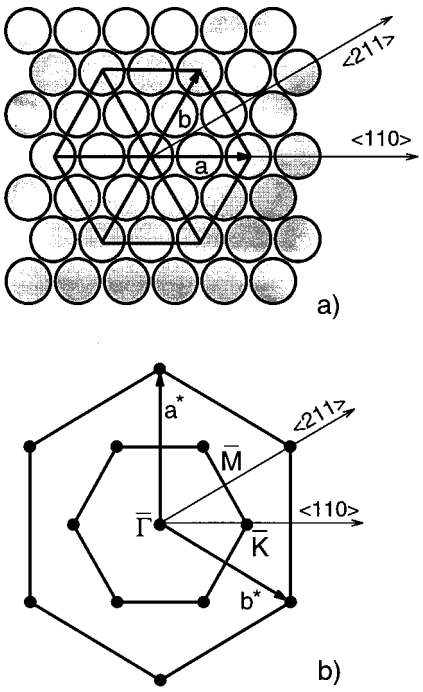

FIG. 1. (a) The real space structure of the sc phase of the $C_{60}(111)$ surface showing the main crystallographic directions. (b) Reciprocal lattice (outer hexagon) together with the first Brillouin zone (inner hexagon). For the sc phase, the length of reciprocal lattice vector is given by $|\mathbf{a}^*|=0.36$ Å^{-1}.

III. MEASUREMENTS OF THE PHONON DISPERSION CURVES

All the inelastic HAS measurements of the surface phonon dispersion curves described in this paper were carried out at $T_{surf}=130$ K, in the low-temperature sc phase of $C_{60}(111)$. Figure 1(a) shows the real-space structure and the surface unit cell of the sc phase. Due to the distinct orientations of the neighboring molecules at $T_{surf}<235$ K, the surface lattice vectors **a** and **b** are equal to the double spacing between the nearest neighbors and can be expressed through the bulk lattice constant by $|\mathbf{a}|=\sqrt{2}|\mathbf{a}_{bulk}|=20.02$ Å. The corresponding reciprocal lattice of the sc phase is shown in Fig. 1(b), where aside from the unit cell (outer hexagon), the first Brillouin zone (inner hexagon) with the main symmetry points $(\bar{\Gamma},\bar{M},\bar{K})$ is also shown. For this phase, the length of reciprocal lattice vector is given by $|\mathbf{a}^*|=0.36$ Å^{-1}. Correspondingly, for the high-temperature fcc phase, the reciprocal space can also be represented by Fig. 1(b) but with reciprocal lattice vectors that are twice as long as those of the sc phase. The corresponding high-symmetry points in the Brillouin zone will be denoted by $\bar{\Gamma}$, $\bar{M}_1$, and $\bar{K}_1$.

Four of a total of 60 measured TOF spectra along the

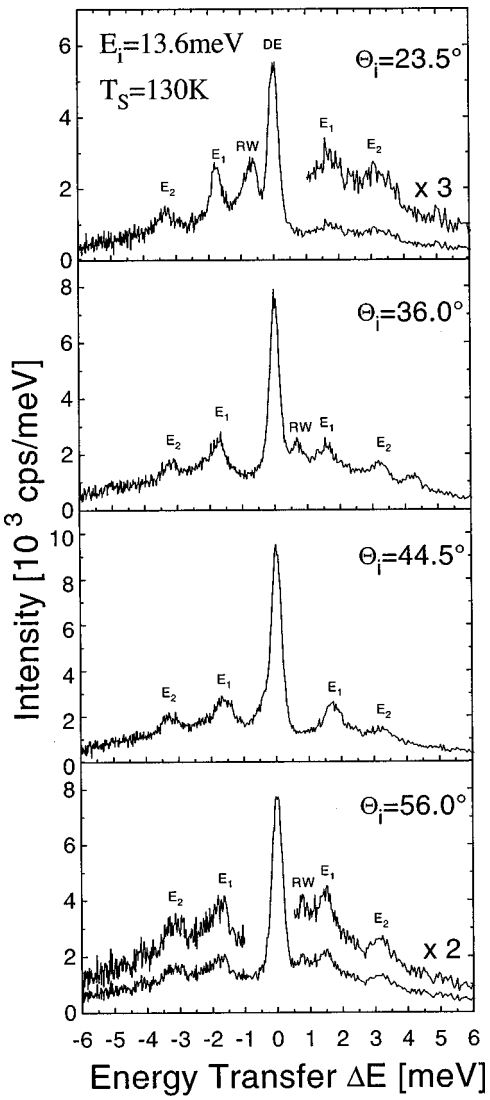

FIG. 2. A series of representative time-of-flight spectra measured along the $C_{60}(111)\langle 110\rangle$ direction at the given incident angles Θ_i for a surface temperature of $T_{\mathrm{surf}}=130$ K and the incident beam energy of 13.6 meV. E_1 and E_2 denote two Einstein modes, while RW is for the Rayleigh wave.

$\langle 110\rangle$ direction, converted to an energy-transfer scale, are displayed in Fig. 2. The diffuse elastic peaks at $\Delta E=0$ meV are attributed to incoherent scattering from symmetry breaking surface defects.[24] The relative signal intensity of these peaks indicates that the surface studied has a relatively low density of defects and that the quality of the surface is comparable with other previously studied single-crystal dielectric and semiconductor surfaces.[25,26]

Besides the diffuse elastic peak, each spectrum has a number of other fairly sharp peaks at positive- and negative-energy transfers. The peaks at the positive-energy side correspond to the annihilation of single phonons, while those on the negative side are due to single phonon excitations. From the energy transfer ΔE of each peak together with the corresponding incident angle Θ_i, the associated parallel momentum transfer ΔK can be calculated from conservation of energy and momentum[25] (scan curve):

$$\hbar\omega=-E_i\left[1-\left(1+\frac{\Delta K}{K_i}\right)^2\frac{\sin^2\Theta_i}{\sin^2\Theta_F}\right], \tag{1}$$

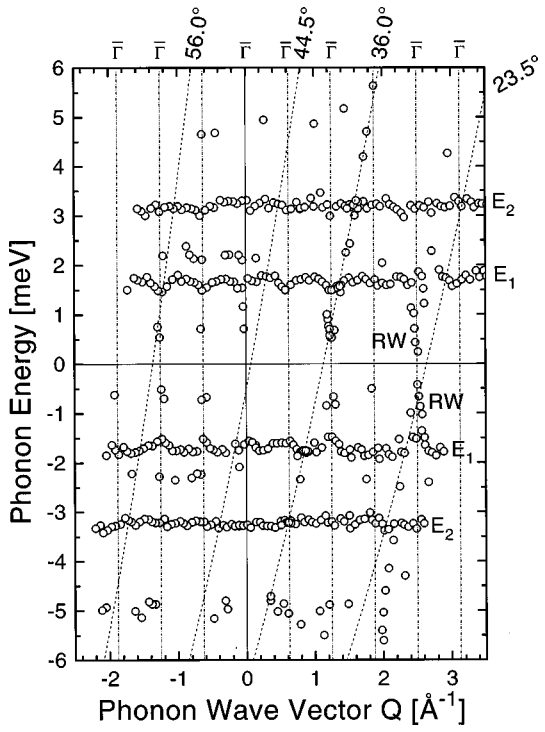

FIG. 3. The surface phonon dispersion curves constructed from all the measured TOF spectra. The scan curves corresponding to the four spectra shown in Fig. 2 are shown as dashed curves. The vertical dashed-dotted lines denote the positions of the Brillouin-zone centers ($\bar{\Gamma}$ points).

where $K_i=k_i\sin\Theta_i$ is the parallel component of the incident beam mom entum, $\Theta_f=90°-\Theta_i$, and E_i is the incident energy of the beam.

The phonon wave vectors together with the corresponding measured phonon energies are presented in Fig. 3 for the $\langle 110\rangle$ direction. This figure also shows the four scan curves corresponding to the incident angles of the TOF spectra in Fig. 2. The vertical dashed-dotted lines denote the positions of the Brillouin zone centers ($\bar{\Gamma}$ points). Two nearly dispersionless Einstein modes E_1 and E_2 with energies of 1.8 ± 0.2 and 3.2 ± 0.2 meV, respectively, were clearly observed in both annihilation and creation. These modes had rather strong features in the TOF spectra and were observed for all measured phonon wave vectors. The energy of E_2 is sufficiently smaller than twice that of E_1 (3.6 meV) so that it is most probably not an overtone of mode E_1. Aside from these Einstein modes, parts of the Rayleigh waves (RW's) were also observed outside the first Brillouin zone. The RW is clearly visible in the TOF spectra shown in Fig. 2 at $\Theta_i=23.5°$, 36.0°, and 56.0°. Furthermore, there are some weak indications (see Fig. 3) for additional Einstein-like phonon modes at around 2.3 and 5.0 meV. However, due to the low signals of these modes, their dispersions along the Brillouin zone cannot be established accurately.

The TOF spectra were also measured along the $\langle 211\rangle$ azimuth. Four of a total of 50 TOF spectra are depicted in Fig. 4. Numerous phonon peaks are clearly visible and can be attributed to the same type of vibrations as in the other azimuth. The peaks are labeled by the same mode notations as in Fig. 2. The corresponding dispersion curves, constructed as described above for the other direction, are presented in

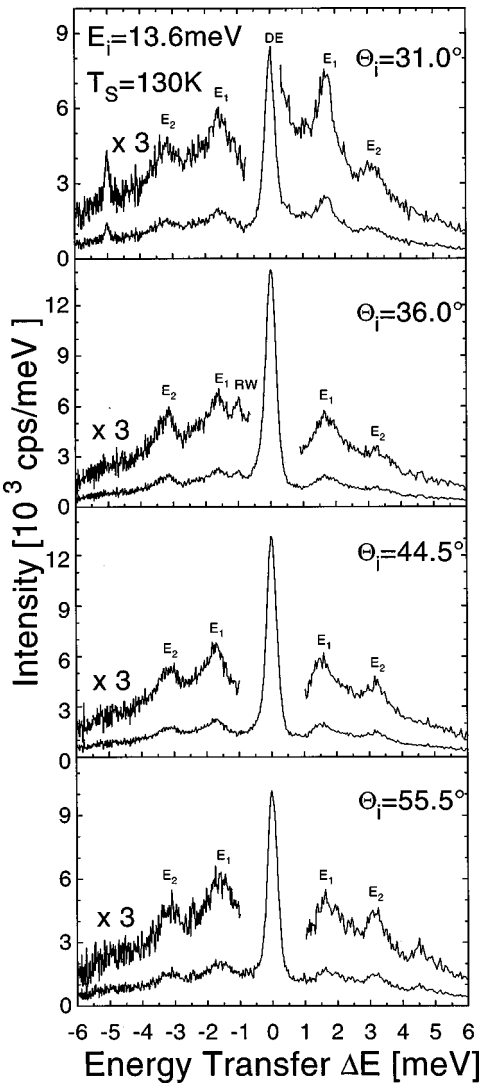

FIG. 4. A series of representative time-of-flight spectra measured along the $C_{60}(111)\langle 211\rangle$ direction at the given incident angles Θ_i. The crystal temperature and the incident beam energies are the same as in the measurements of Fig. 2.

Fig. 5 in an extended zone diagram. The vertical dashed-dotted lines indicate Γ points. The two modes E_1 and E_2 are also very pronounced for all phonon wave vectors, and some parts of the RW can also be seen. These measured dispersion curves will be discussed in Sec. IV in connection with the results of the calculations.

IV. CALCULATION OF THE DISPERSION CURVES

The surface phonon dispersion curves of $C_{60}(111)$ films were calculated with the Girifalco intermolecular potential.[19] This simple, radial potential is obtained by integrating the 12-6 Lennard-Jones interactions $c_{12}/r^{12}-c_6/r^6$, where r is the distance between two parts in adjacent C_{60} spheres of radius 3.55 Å. The two parameters (c_{12} and c_6) of the potential were adjusted to reproduce the lattice parameter and the sublimation energy of the C_{60} fullerite at room temperature. This model is unable to reproduce the orientational-ordering transition involving the librational degrees of freedom since the molecules are approximated by smooth noncorrugated

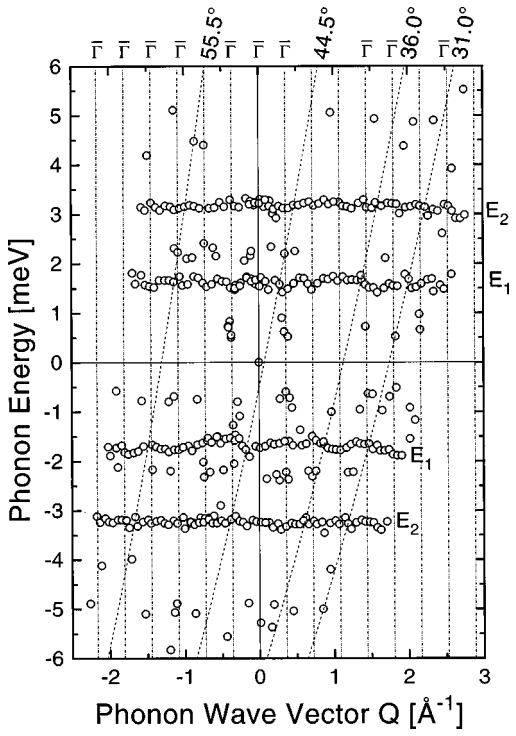

FIG. 5. The surface phonon dispersion curves together with the scan curves (dashed lines) corresponding to the four TOF spectra shown in Fig. 4. The vertical dashed-dotted lines denote the positions of the Brillouin-zone centers ($\bar{\Gamma}$ points).

spheres. As a consequence, the sc and fcc structures are energetically equivalent, but the first Brillouin zone of the sc phase is folded in order to account for the reduced size of the Brillouin zone.

The Girifalco model reproduces fairly well the elastic constants of solid C_{60} deduced from a more sophisticated intermolecular potential.[9] However, these constants seemingly overestimate the Brillouin scattering data[18] by as much as 60%, and this might exagerate the acoustic phonon frequencies by 25%. By contrast the highest phonon frequency given by the Girifalco potential for bulk C_{60} is 7.0 meV, in good agreement with inelastic neutron data.[11]

Figure 6(a) shows the phonon dispersion curves computed for a (111) film of 50 layers of C_{60} with the (1×1) unit cell of the fcc structure. Of special interest is the pair of Rayleigh waves located at the two free surfaces that rapidly coalesce into a single branch for Q away from the $\bar{\Gamma}$ point and culminates to 3.2 meV at the K_1 point. In order to compare the calculations with the low-temperature experimental data, the sc (2×2) unit cell was used to calculate the surface character of the phonons. The results are shown in Fig. 6(b) for a 12-layer film where the gray scale represents the sum of the square amplitudes on the four molecules composing the topmost layer and projected along the normal vector at the surface ($SP_\perp$ polarization). This polarization was chosen since with HAS the probability for exciting the $SP_\perp$ modes is usually greater than for exciting the $SP_\parallel$ mods,[27] whereas the excitation of the shear horizontal modes is forbidden along high-symmetry directions.[25]

Doubling the unit cell has the important effect that the Rayleigh wave is folded back into the reduced first-Brillouin zone and, thus, gives rise to a nearly flat band at around 3

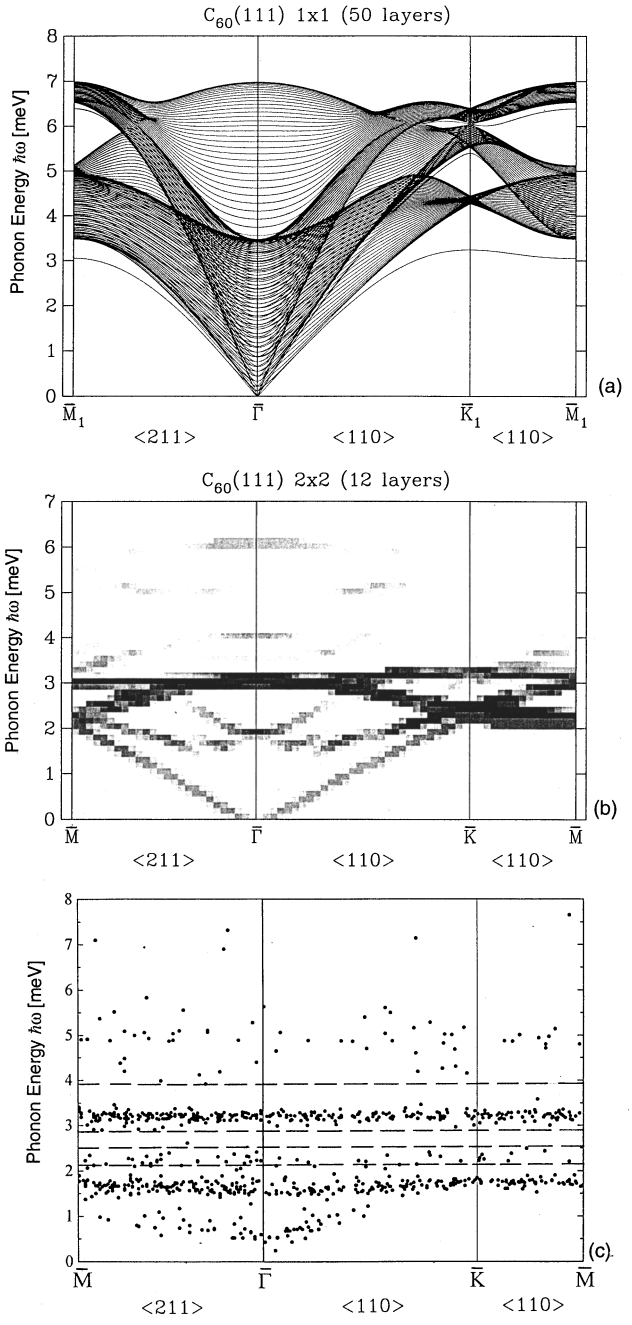

FIG. 6. (a) The surface phonon band structures computed for a slab of 50 (111) layers of C_{60} in the extended Brillouin zone corresponding to the high-temperature fcc structure. (b) Surface phonon characters with $SP_{\perp}$ polarization computed in the reduced Brillouin zone corresponding to the low-temperature sc (2×2) structure. The band structures (a) and (b) were obtained with the Girifalco potential on relaxed structures of the films. The labels $\bar{K}_1$ and $\bar{M}_1$ in (a) are the high-symmetry points of the first Brillouin zone generated by the fcc structure, and $\bar{K}$ and $\bar{M}$ in (b) are the corresponding points in the reduced zone shown in Fig. 1(b). (c) Experimental dispersion curves deduced from the HAS spectra recorded at 130 K, with the horizontal lines indicating the energies of the bulk librons listed in Table I.

meV all along the high-symmetry directions. Of course, in the real (2×2) structure, the four molecules in each (111) layer are not equivalent and folding the band structure of the fcc cell is only an approximation. However, it is believed that most of the important effects are already accounted for by the folding.

TABLE I. The energies (meV) of the libron modes determined in bulk C_{60} by Raman spectroscopy and neutron inelastic scattering, extrapolated to 130 K using the anharmonicity coefficient $\chi_{\text{bulk}} = 0.017$, are compared to the E_1 and E_2 energies measured at the same temperature by HAS.

Raman[a]	Neutron[b]	HAS[c]
2.0	2.1	1.8
2.4	2.6	
2.8	2.8	
2.8	2.9	3.2
3.8	4.0	

[a]References 1 and 12.
[b]References 1 and 11.
[c]Present work.

The HAS dispersion curves of Figs. 3 and 5 are plotted in Fig. 6(c) in the reduced zone corresponding to the sc phase. The modes E_1 and E_2 are nearly dispersionless with energies of about 1.8 and 3.2 meV, while the points arising on both sides of the $\bar{\Gamma}$ point are attributed to the Rayleigh wave. For comparison, the horizontal dashed lines show the frequencies of the bulk C_{60} librons measured by Raman spectroscopy and neutron inelastic scattering (see Table I).

Even though the calculated phonon bands of Fig. 6(b) do not acount for the librational modes, they nicely reproduce several of the experimental features summarized in Fig. 6(c). The folding of the Rayleigh wave itself might suffice to explain dispersionless data, especially since the folded branch is found right at the same energy as the E_2 mode. However, the frequencies of the E_1 and E_2 mode depend on the temperature, due to the anharmonicity of the observed vibrations as discussed in the next section. In addition, the frequency of the Rayleigh wave at the $\bar{K}_1$ point may be overestimated, since the calculations yield a Rayleigh wave phase velocity of 1850 m/s along $\langle 211\rangle$, which is about 30% higher than the experimental value determined by surface Brillouin scattering.[18] Taking this correction into account would shift the folded Rayleigh branch down to 2.4 meV, between the E_1 and E_2 modes where indeed some experimental points are found.

V. ANHARMONICITY OF THE SURFACE PHONONS

To obtain information on the anharmonicity of the phonons on the $C_{60}(111)$ surface, the TOF spectra were measured for different substrate temperatures between 130 and 270 K. The measurements were performed along the $\langle 110\rangle$ direction at an incident angle $\Theta_i = 36°$, with an incident beam energy of 13.6 meV at different surface temperatures. Figure 7 exhibits the eight measured TOF spectra. The wave vector transfer associated with the elastic peak is $\Delta K = 1.12\ \text{Å}^{-1}$. At higher temperatures, multiphonon scattering results in a reduction of the single phonon peak intensities and in an increase in the background. At $T_{\text{surf}} = 250$ K, the single phonon peaks are no longer detectable. For the same

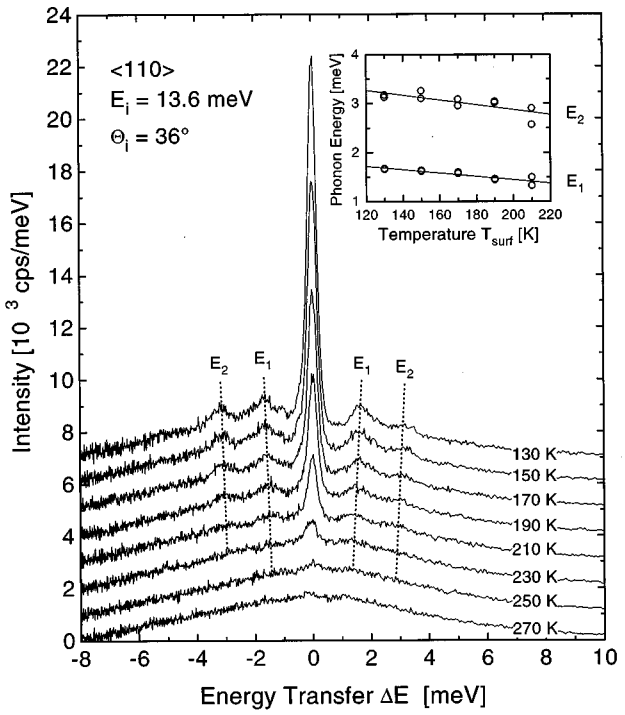

FIG. 7. TOF spectra measured from the $C_{60}(111)$ surface along the $\langle 110 \rangle$ directions for various surface temperatures. The decrease with temperature of the librational modes is plotted in the inset.

reason the diffuse elastic peak also decreases with the temperature.[21]

From Fig. 7 it is apparent that the peaks corresponding to modes E_1 and E_2 shift towards lower frequencies with increasing temperature. The inset in Fig. 7 shows the temperature dependence of both modes. As can be seen from this plot, the energy decay for both modes can be fitted with linear functions of the form $\Delta E = a + bT_{\mathrm{surf}}$. The linear regression for the E_1 and E_2 modes yields $a_1 = 2.13 \pm 0.1$ meV and $b_1 = -3.4 \pm 0.5$ μeV/K, and $a_2 = 3.85 \pm 0.25$ meV and $b_2 = -5.0 \pm 1.5$ μeV/K, respectively. The a parameters correspond to the phonon frequencies extrapolated to the surface temperature of 0 K, while the slope coefficients b_1 and b_2 are related to the anharmonicity constants of the C_{60} surface.

Anharmonic effects on surfaces have been discussed by Benedek and Toennies[28] and have been previously observed on several clean metal surfaces as well as on several adsorbate layers.[29] In an anharmonic potential well, the energy eigenvalues are not equidistant, and at higher temperatures the quantum transitions $n \rightarrow n+1$ with large n make increasing contributions, thus, leading to the asymmetric broadening and shift of the phonon peak. To a first approximation,[28] the anharmonic shift of the phonon energies is proportional to the harmonic energy of the oscillator $\hbar\omega_0$ and is given by

$$E = \hbar\omega(T_{\mathrm{surf}}) = \hbar\omega_0 - \chi_e \hbar\omega_0 (2n_0 + 1), \tag{2}$$

where χ_e is the anharmonicity constant and n_0 is the temperature-dependent occupation number for Bose statistics: $n_0 = [\exp(\hbar\omega/k_B T) - 1]^{-1}$. Since the surface temperature range used in the present measurements is such that $\hbar\omega_0 \ll k_B T$, the temperature dependent energy shift $\Delta E(T)$ can be expanded and simplified to the following form:

$$\Delta E = -\chi_e \hbar\omega_0 (2n_0 + 1) = -2\chi_e k_B T. \tag{3}$$

Thus, comparing this equation with the linear regression fits of the $(\Delta E - T_{\mathrm{surf}})$ curves, shown in the insert of Fig. 7, the anharmonicity constants χ_{e1} and χ_{e2} for the two observed librational modes can be easily calculated:

$$\chi_{e1} = -\frac{b_1}{2k_B} = 0.020 \pm 0.002,$$

$$\chi_{e2} = -\frac{b_2}{2k_B} = 0.029 \pm 0.009. \tag{4}$$

These values are comparable to the anharmonicity coefficients of 0.0175 and 0.024 measured for the Rayleigh wave on Cu(001) and Al(111) surfaces, respectively.[30]

In C_{60}, the energy shift with the temperature of the librational modes has already been observed in the bulk by means of neutron[10] and Raman[12] scatterings. Fitting these data with a linear regression results in the bulk anharmonicity constant $\chi_{e1}^{\mathrm{bulk}} = 0.017 \pm 0.001$, which is a factor 0.88 smaller that that of the surface mode E_1. The enhanced surface anharmonicity can be caused by a number of factors,[28] the most important of which probably is the reduced coordination of the surface molecules as compared to the bulk.

VI. CONCLUSION

High-resolution elastic and inelastic helium atom scattering experiments have been carried out to investigate the low-frequency vibrational dynamics of the C_{60} films grown epitaxially on the cleaved GeS(001) surface. The phonon dispersion curves of the sc phase of $C_{60}(111)$ were measured at $T_{\mathrm{surf}} = 130$ K along two high-symmetry directions. Three modes were clearly identified in the time-of-flight spectra, two of them being dispersionless (E_1 and E_2 modes), while the other one could unambiguously be attributed to the surface acoustic Rayleigh wave. The energies of the E_1 and E_2 mode at $T_{\mathrm{surf}} = 130$ K are 1.8 and 3.2 meV. They deviate by ± 0.3 meV from the frequencies of the libron modes determined for bulk C_{60} by Raman and neutron inelastic scattering experiments (see Table I). By measuring the temperature dependence of the libron energies, the surface anharmonicity constants were found to be about 12% higher than the corresponding bulk ones.

Surface phonon dispersion curves were also calculated on the basis of the Girifalco intermolecular potential, with the C_{60} molecules being approximated by smooth uncorrugated spheres. The calculations demonstrated that the Rayleigh mode, when folded back to the first Brillouin zone of the sc phase, gives rise to a nearly dispersionless mode at around 3.2 meV, which might contribute to the measured E_2 mode. However, renormalizing the potential parameters to fit the phase velocity of the Rayleigh wave measured by surface Brillouin scattering at the $\bar{\Gamma}$ point could lower the energy of the folded branch by 0.8 meV and, therefore, the predicted

coincidence with the E_2 mode may be accidental. In closing it is worth recalling that the calculations were performed in the harmonic approximation and no temperature effects were included. Furthermore, the force constants were taken to be the same as in the bulk, which in fact might differ at the surface. For these reasons, a more sophisticated approaches would be desirable in order to fully understand these new experiments.

ACKNOWLEDGMENTS

P.S. was supported by the Belgian PAI/IUAP program No. P4/10.

[1] T. Pichler, M. Haluska, J. Winter, R. Winkler, B. Burger, M. Hulman, and H. Kuzmany, Fullerene Sci. Technol. **4**, 227 (1996).
[2] G. Dresselhaus, M. S. Dresselhaus, and P. Eklund, Phys. Rev. B **45**, 6923 (1992).
[3] X. P. Li, J. P. Lu, and R. M. Martin, Phys. Rev. B **46**, 4301 (1992).
[4] T. Yildrim and A. B. Harris, Phys. Rev. B **46**, 7878 (1992).
[5] W. I. F. David, R. M. Ibberson, J. C. Matthewman, K. Prassides, T. J. S. Dennis, J. P. Hare, H. W. Kroto, R. Taylor, and D. R. M. Walton, Nature (London) **353**, 147 (1991).
[6] A. Goldoni, C. Cepek, and S. Modesti, Phys. Rev. B **54**, 2890 (1996).
[7] Y. Yoneda, K. Sakaue, and T. Terauchi, J. Phys.: Condens. Matter **9**, 2851 (1997).
[8] A. Glebov, V. Senz, J. P. Toennies, and G. Gensterblum, J. Appl. Phys. **82**, 2329 (1997).
[9] J. Yu, R. K. Kalia, and P. Vashishta, Appl. Phys. Lett. **63**, 3152 (1993); J. Yu, L. Bi, R. K. Kalia, and P. Vashishta, Phys. Rev. B **49**, 5008 (1994).
[10] D. A. Neumann, J. R. D. Copley, W. A. Kamitakahara, J. J. Rush, R. L. Cappalletti, N. Coustel, J. E. Fisher, J. P. McCauley, A. B. Smith, K. M. Creegan, and D. M. Cox, J. Chem. Phys. **96**, 8631 (1992).
[11] L. Pitschovius, B. Renker, F. Gompf, R. Heid, S. L. Chaplot, M. Haluska, and H. Kuzmany, Phys. Rev. Lett. **69**, 2662 (1992).
[12] P. J. Horoyski, M. L. W. Thewalt, and T. R. Anthony, Phys. Rev. B **52**, 6951 (1995).
[13] W. Que and M. B. Walker, Phys. Rev. B **48**, 13 104 (1993).
[14] P. J. Horoyski and M. L. W. Thewalt, Phys. Rev. B **48**, 11 446 (1993).
[15] S. A. Fitzgerald and A. J. Sievers, Phys. Rev. Lett. **70**, 3175 (1993).
[16] S. Huant *et al.*, Phys. Rev. Lett. **69**, 2666 (1992).
[17] D. Schmicker, S. Schmidt, J. G. Skrofonick, J. P. Toennies, and R. Vollmer, Phys. Rev. B **44**, 10 995 (1991).
[18] D. Fioretto, G. Carlotti, G. Socino, S. Modesti, C. Cepek, L. Giovannini, O. Donzelli, and F. Nizzoli, Phys. Rev. B **52**, R8707 (1995).
[19] L. A. Girifalco, J. Phys. Chem. **96**, 858 (1992).
[20] J. P. Toennies and R. Vollmer, Phys. Rev. B **44**, 9833 (1991).
[21] J. P. Toennies, in *Surface Phonons*, edited by W. Kress and F. W. de Wette, Springer Series of Surface Sciences Vol. 21 (Springer, Berlin, 1990), Chap. 5.
[22] Provided by G. A. Sawatzky, University of Groningen.
[23] G. Gensterblum, K. Hevesi, B. Y. Han, L. M. Yu, J. J. Pireaux, P. A. Thiry, R. Caudano, A. A. Lucas, D. Bernaerts, S. Amelinckx, G. Van Tendeloo, G. Bendele, T. Buslaps, R. L. Johnson, M. Foss, R. Feidenhans'l, and G. Le Lay, Phys. Rev. B **50**, 11 981 (1994).
[24] A. Glebov, J. R. Manson, J. G. Skofronick, and J. P. Toennies, Phys. Rev. Lett. **78**, 1508 (1997).
[25] A. Glebov, W. Silvestri, J. P. Toennies, G. Benedek, and J. G. Skofronick, Phys. Rev. B **54**, 17 866 (1996).
[26] G. Lange and J. P. Toennies, Phys. Rev. B **53**, 9614 (1996).
[27] J. R. Manson and V. Celli, Surf. Sci. **24**, 495 (1971).
[28] G. Benedek and J. P. Toennies, Phys. Rev. B **46**, 13 643 (1992).
[29] A. Graham, F. Hofmann, and J. P. Toennies, J. Chem. Phys. **104**, 5311 (1995).
[30] M. Gester, D. Kleinhesselink, P. Ruggerone, and J. P. Toennies, Phys. Rev. B **49**, 5777 (1994).